Available online at www.sciencedirect.com

ScienceDirect

Procedia Structural Integrity 9 (2018) 64–70

Structural Integrity Procedia

www.elsevier.com/locate/procedia

IGF Workshop "Fracture and Structural Integrity"

Experimental and numerical analysis of TIG-dressing applied to a steel weldment

P. Ferro[a*], F. Berto[b], F. Bonollo[a], R. Montanari[c*]

[a] *Department of Engineering and Management, University of Padova, Stradella San Nicola 3, 36100 Vicenza (Italy)*
[b] *NTNU, Department of Engineering Design and Materials, Richard Birkelands vei 2b, 7491, Trondheim (Norway)*
[c] *Department of Industrial Engineering, University of Rome Tor Vergata, Via del Politecnico 1, 00133, Rome (Italy)*

Abstract

Fatigue strength of welded joints is controlled above all by notch defects such as weld toe and weld root that act as stress concentrators. This is the reason why over the last years different post-weld fatigue improvement techniques have been developed with the main propose of reducing geometrical discontinuities. Among these, TIG-dressing is the most used because of its simplicity and effectiveness in lowering the residual stress concentration. By this process the weld toe is re-melted to provide a smoother transition between the plate and the weld crown and to beneficially modify the residual stress redistribution. However, because of the intrinsic difficulty to numerically simulate the TIG-dressing process due to the high coupling between fluid and mechanical analysis, the effects of a weld toe remelting in terms of residual stress redistribution is hardly quantified in literature. The present paper is aimed to analyse the influence of TIG-dressing process on metallurgical and mechanical properties of a steel T-joint. Finally, a numerical model, recently published in literature, was used to quantified the residual stress redistribution.

Peer-review under responsibility of the Gruppo Italiano Frattura (IGF) ExCo.

Keywords: Welding; TIG-dressing; Modeling; Numerical simulation; Residual stress, Phase transformation

* Corresponding author. Tel.: +39-0444-998769; fax: +39-0444-998888.
E-mail address: paolo.ferro@unipd.it

2452-3216
Peer-review under responsibility of the Gruppo Italiano Frattura (IGF) ExCo.
10.1016/j.prostr.2018.06.012

1. Introduction

It is recognised that fatigue strength of welded joints doesn't increase with the increase of their parent-metal static strength. The low fatigue strength of welded joints is due to different reasons, the most important of which is the stress concentration at the weld toe or weld root. For this reason, some techniques, aimed to improve the fatigue strength of welded joints, were developed [Kirkhope et al., (1999)]. They act mainly on two aspects: 1) the geometrical variation of the weld bead and 2) the reduction of the stress concentration factors. Among these techniques, the TIG-dressing is probably the most used and consists in the re-melting of the weld toe by means of the TIG heat source (without filler metal) [Haagensen et al., (2001); van Es et al., (2013)]. Such operation promotes a smoother transition between the plate and the weld crown and thus a reduction of the stress concentration factor as well as a residual stress redistribution. Unfortunately, even if numerical models of welding and TIG-dressing processes were developed in the last years [Ferro et al. (2005); Ferro et al. (2006); Akbari and Miresmaeili, (2008); Das and Cleary, (2016); Vemanaboina et al. (2014); Hildebrand et al. (2006); Ferro et al., (2010)], it is very hard to quantify such effects by numerical simulations because they are still highly time and cost expensive. In particular, the numerical simulation of TIG-dressing process is particularly complex because it requires a high coupling between thermo-metallurgical-fluid analysis and mechanical analysis. The weld bead geometrical variation induced by re-melting is influenced by the weldment distortions during TIG-dressing and vice-versa. For this reason, it was recently published in literature a numerical model of the TIG-dressing process that simplifies a lot the computation by using the activation-deactivation function of elements [Ferro et al., (2017)]. In this way, it is possible to avoid the fluid analysis, but the weld toe geometrical variation has to be 'a priori' known by means of welding and TIG-dressing trials. Such model is applied in this work to a real weldment and the results in terms of metallurgical and mechanical properties are compared and discussed

2. Materials, Geometry and Experiments

The steel weldment analysed consists of two plates, 12 mm thick, joined together by means of two plates, 6 mm thick, fillet welded (Fig. 1).

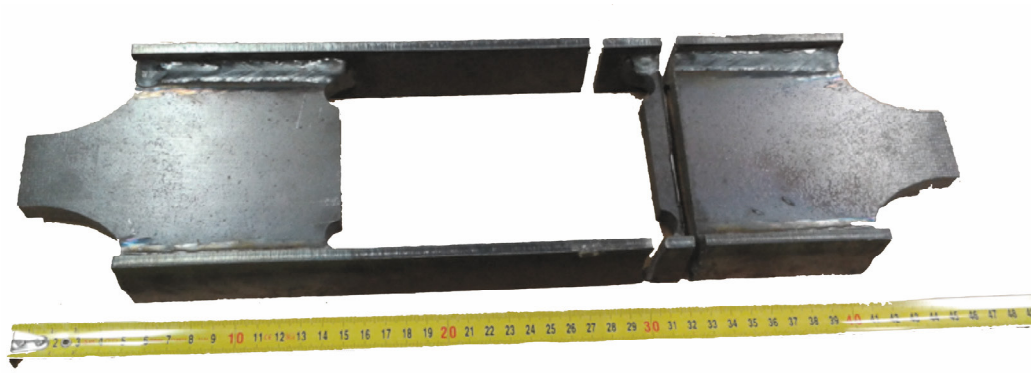

Fig. 1. Investigated Weldment

The chemical analysis coming from the average values of quantometer measurements is summarized in Tab. 1.

Table 1. Chemical composition of the plates (wt%)

	Fe	C	Si	Mn	P	S	Ni	Al	Cu
Parent Metal (plates 12 mm thick)	Bal.	0,1223	0,0101	1,3467	0,0168	0,0161	0,0253	0,0378	0,0502
Parent Metal (plates 6 mm thick)	Bal.	0,0756	0,0128	1,1575	0,0143	0,0073	0,0056	0,0285	0,0087
Fusion Zone	Bal.	0,0892	0,4453	1,3800	0,0186	0,0142	0,0181	0,0083	0,0549

Some samples were cut from the weldment for the metallographic analysis carried out by means of optical microscope (OM) and Environmental Scanning Electron Microscope (ESEM). Finally, Vickers micro-hardness profiles were also obtained as support to the microstructure interpretation. Unfortunately, no information was available about welding parameters.

3. Numerical Model

The geometry of the numerical model and the reference system used to plot the residual stress field of the final joint, according to the blunt V-Notch theory, are shown in Fig. 2.

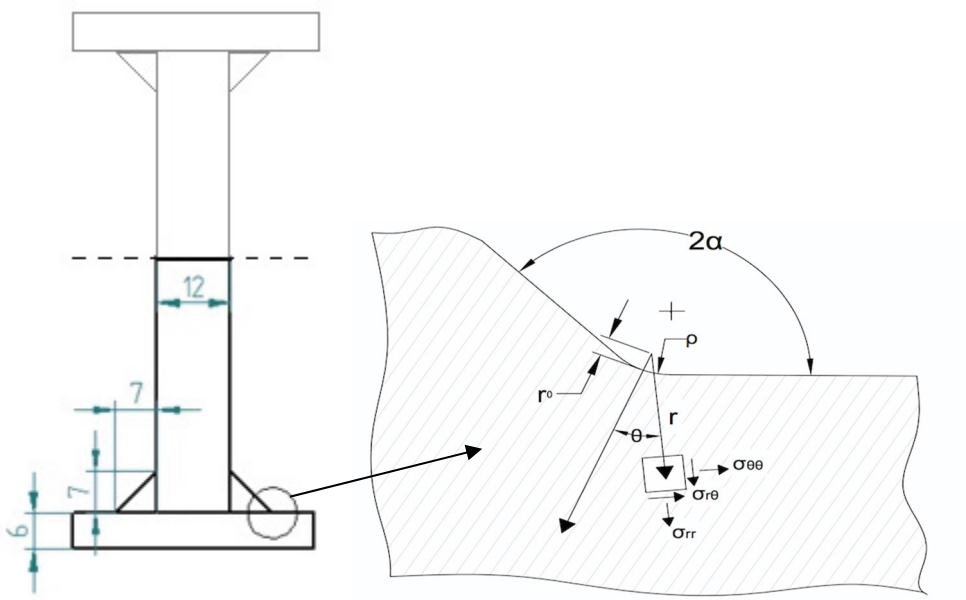

Fig. 2. Schematic of the modelled geometry (mm)

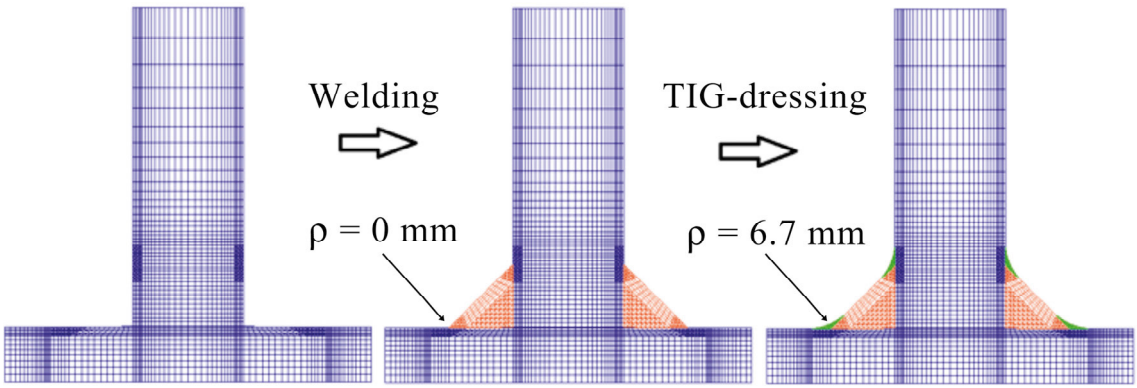

Fig. 3. Mesh of the model. Number of elements: 5436. The edge of the smallest element in the singularity zone has a dimension of $5*10^{-4}$ mm.

The weld toe was modelled with a V-notch angle (2α) equal to 135° [Ferro et al., (2006)]. The toe-radius (ρ) is equal to 0 mm in the as-welded condition and 6.7 mm after TIG-dressing treatment. This last value was obtained by

averaging the measurements carried out on real samples. Fig. 3 shows the mesh with the groups of elements used to simulate the geometry variation induced by welding. In particular, the orange elements groups represent the beads that are activated during welding simulation while the green elements groups are activated during the TIG-dressing FE analysis in order to simulate the smoothing effect induced by the process. It is noted that a high-density mesh is used near the weld toe in order to capture the residual stress singularity induced by welding. The different welding and TIG-dressing operations were sequentially performed according to Fig. 4. Thermo-metallurgical and mechanical properties of both filler and parent metals were taken from Sysweld data-base). Filler and parent metals alloys were chosen according to chemical compositions reported in Tab. 1.

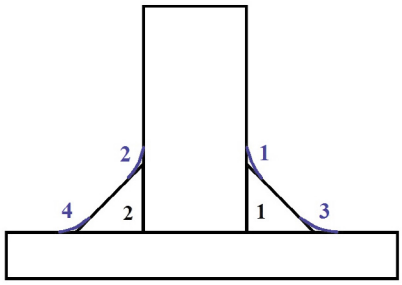

Fig. 4. Welding and TIG-dressing operations sequence.

In including metallurgical effects in the present analysis the following microstructural constituents were considered: martensite, bainite, ferrite-pearlite, tempered martensite, tempered bainite and austenite. They were modelled by means of the Leblond-Devaux [Leblond and Devaux, (1984)] and Koistinen-Marburger [Koistinen and Marburger, (1959)] equations according to their diffusional or non-diffusional feature. The simplifying assumptions were made that tempered bainite has the same properties as ferrite and that tempered martensite is similar in properties to bainite. The heat source was modelled using a double ellipsoid power density distribution function given by Goldak et al. [Goldak et al., 1984] (Eq. 1) that has been used previously in published literature for arc welding simulation [Ferro et al., 2010].

$$q_g(x,y,t) = \frac{6\sqrt{3} f_{1,2} Q}{\pi\sqrt{\pi} abc_{1,2}} e^{-\frac{3x^2}{a^2}} e^{-\frac{3y^2}{b^2}} e^{-\frac{3[v(\tau-t)]^2}{c_{1,2}^2}} \quad (1)$$

The meaning of the symbols in Eq. (1) and their values are summarized in Tables 2 and 3.

Table 2 - Goldak's source parameters. * indicates that the value used depends on the process (see Table 3). The high value of τ for TIG-dressing includes the time necessary for the weld to cool to room temperature after welding

Q*	Power Input[W]	*
η	Efficiency	0.64
Q	Absorbed power [W], with Q=ηQ*	-
a	Molten pool dimensions [mm]	*
b		*
c_1		2.3
c_2		7.9
f_1	Constants for the energy distribution of the heat flux	0.6
f_2		1.4
v	Welding speed [mms^{-1}]	2
	TIG-dressing speed[mms^{-1}]	3
τ	Total duration of time before the welding source has traversed the transverse cross section of the plate [s]	*

Table 3 – Heat source parameters given as a function of the weld process.

	Q* [W]	a [mm]	b [mm]	τ [s]
TIG welding 1	4500	8	11	5
TIG welding 2	4500	8	11	3005
TIG-dressing 1	960	6	3	6005
TIG-dressing 2	960	6	3	7065
TIG-dressing 3	960	6	3	8125
TIG-dressing 4	960	6	3	9185

The molten-remolten effect was simulated by incorporating a function that clears the history of an element once the temperature exceeds the melting temperature, which was taken as 1500°C. Radiative heat loss (using the Stephan-Boltzmann law) and convective heat loss (using a convective heat transfer coefficient equal to 25 W/m^2K) were applied at the boundary (external surfaces) of the plates to be joined. In the mechanical computation the weldment was considered isostatically clamped. Finally, a sequentially coupled thermo-metallurgical and mechanical analysis was performed by using the numerical code Sysweld®.

4. Results and discussion

Fig. 5 shows the temperature distribution at the point when the fusion zone has its maximum width with the fusion zone (FZ) being shown in red. It also shows the macrograph of the joint cross section after TIG-dressing (Fig. 5c). The proportional distributions of phases after cooling with a comparison with experimental results are shown in Fig. 6. According to numerical simulation, each FZ is characterised by a mixture of allotriomorphic and Widmanstatten ferrite probably due a combination between the low carbon content (Tab. 1) and the cooling rate in that zone. The heat-affected zone (HAZ) is instead characterized by bainite (about 50%) and tempered bainite (about 50%). SEM micrograph (Fig.6) and micro-hardness measurements (not reported in this work) confirm the obtained numerical results.

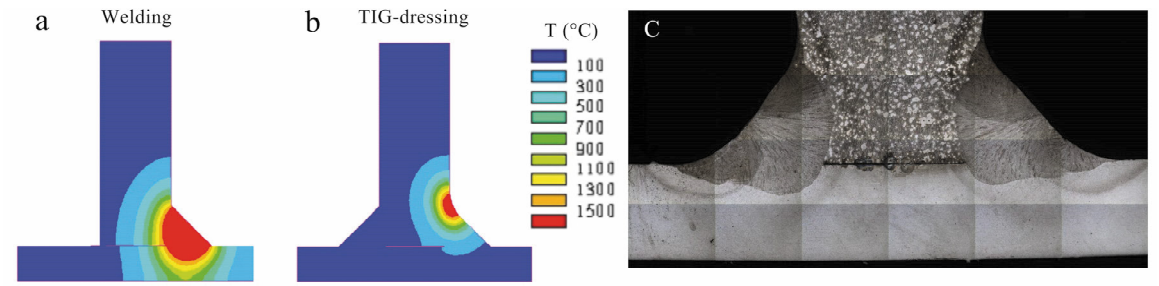

Fig. 5. FZ shape induced during a) TIG welding and b) TIG-dressing, respectively, and c) macrograph of the joint after TIG-dressing operations.

Even if a 2D model is not able to correctly capture the residual stress distribution in the welded joint, a qualitative estimation may be useful to understand the effect of TIG-dressing on the residual stress redistribution. Fig. 7 shows the tensile asymptotic distribution of the residual stress ($\sigma_{\theta\theta}$ component) in the as-welded joint. As described in literature [Ferro et al., (2006); Ferro and Petrone, (2009); Ferro, (2014)], if the weld toe is modelled as a sharp V-notch angle, the residual stress field is singular and follows the Williams's solution [Williams, (1952)].
After TIG-dressing, the residual stress near the weld toe redistributes becoming compressive with a huge reduction of its local concentration (Fig. 8). Such effects are in agreement with the improved fatigue strength observed in welded joints subjected to TIG-dressing.

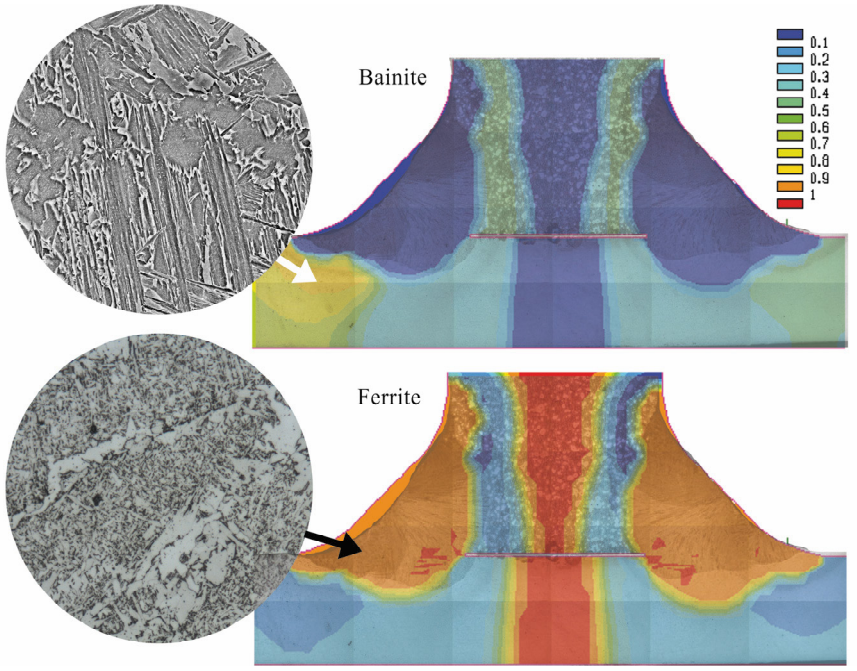

Fig. 6. Phase proportion after TIG-dressing: comparison between experimental and numerical results

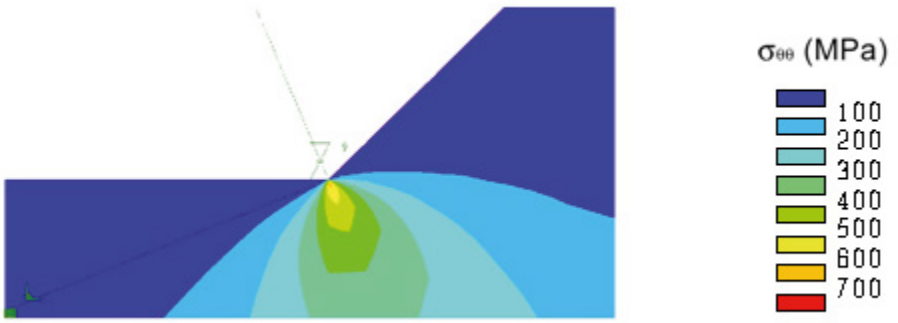

Fig. 7. Stress distribution near the weld toe of the as-welded joint

5. Conclusions

A carbon steel waldment subjected to TIG-dressing was studied by means of experimental and numerical analyses. The TIG-dressing process modified the geometry of the weld toe providing a smoother transition between the plate and the weld crown. Numerical and experimental results were found in good agreement. In particular, allotriomorphic and Witmanstatten ferrite were found in the FZ while bainite and tempered bainite in the HAZ. As expected, the re-melting of the weld toe promoted a beneficial residual stress re-distribution with a huge reduction of the concentration factor and an inversion of its sign, from positive to negative. The simplified numerical model proposed and based on the activation/deactivation of elements instead of fluid analysis, may be useful to rapidly estimate the effects of welding and TIG-dressing operations sequence on the residual stress distribution of the joint.

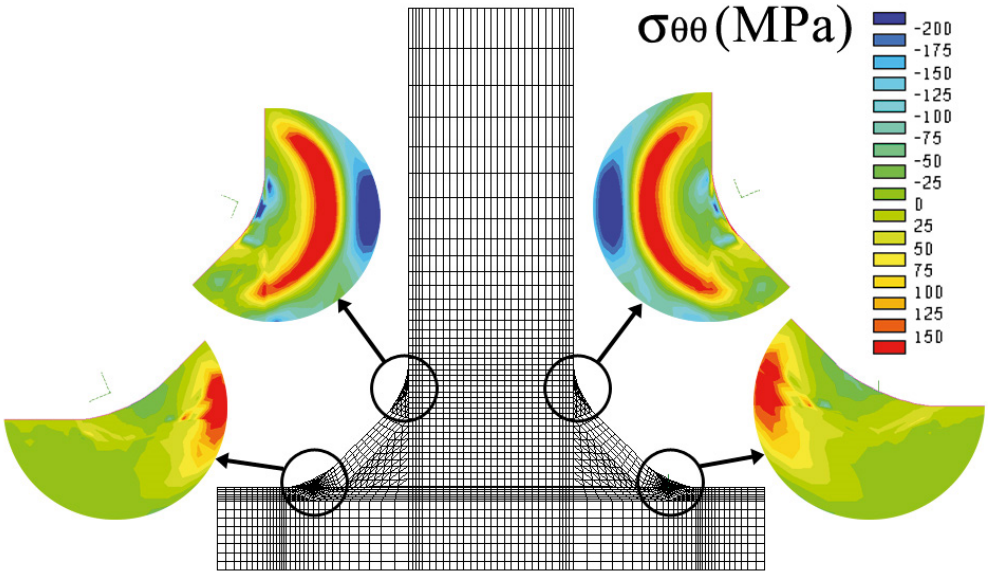

Fig. 8. Residual stress distribution ($\sigma_{\theta\theta}$ component, Fig. 2) after TIG-dressing.

References

Akbari, S.A.A. and Miresmaeili, R., 2008. Experimental and numerical analyses of residual stress distributions in TIG welding process for 304L stainless steel. *Journal of Materials Processing Technology* 208, 383–394.

Das R. and Cleary, P.W., 2016. Three-dimensional modelling of coupled flow dynamics, heat transfer and residual stress generation in arc welding processes using the mesh-free SPH method. *Journal of Computational Science* 16, 200-216.

Ferro P., Porzner, H., Tiziani, A., Bonollo, F., 2006. The influence of phase transformations on residual stresses induced by the welding process - 3D and 2D numerical models. *Modelling Simul. Mater. Sci. Eng.* 14, 117-136.

Ferro, P., 2014. The local strain energy density approach applied to pre-stressed components subjected to cyclic load. *Fatigue Fract Eng Mater Struct* 37, 1268–1280.

Ferro, P., Berto, F., James, M.N., 2017. A simplified model for TIG-dressing numerical simulation. Modelling Simul. Mater. Sci. Eng. 25, 035012

Ferro, P., Berto, F., Lazzarin, P., 2006. Generalized stress intensity factors due to steady and transient thermal loads with applications to welded joints. Fatigue and Fracture of Engineering Materials and Structures 29(6), 440-453

Ferro, P., Bonollo, F., Tiziani, A., 2005. Laser welding of copper-nickel alloys: a numerical and experimental analysis. *Science and Technology of Welding and Joining,* 5(3), 299-310.

Ferro, P., Bonollo, F., Tiziani, A., 2010. Methodologies and experimental validations of welding process numerical simulation. Int J Computational Materials Science and Surface Engineering 3, 114-32.

Ferro, P., Petrone, N., 2009. Asymptotic thermal and residual stress distributions due to transient thermal loads. *Fatigue Fract Eng Mater Struct* 32, 936–948.

Goldak, J., Chakravarti, A. and Birbby, M., 1984. A new finite element model for welding heat sources. Metallur Trans B 15b, 299–305.

Haagensen, P.J. and Maddox, S.J., 2001. IIW recommendations on post weld improvement of steel and aluminium structures. IIW Commission XIII, July 2001.

Hildebrand, J., Starcevic, I., Werner, F., Heinemann, H. and Köhler, G., 2006. Numerical simulation of TIG-dressing of welded joints. Joint International Conference on Computing and Decision Making in Civil and Building Engineering. June 14-16 – Montreal, Canada.

Kirkhope, K.J., Bell, R., Caron, L., Basu, R.I. and. Ma, K-T, 1999. Weld detail fatigue life improvement techniques. Part 1: review. *Marine Structures* 12, 447-474.

Koistinen, D.P. and Marburger, R.E., 1959. A general equation prescribing extent of austenite-martensite transformation in pure iron-carbon alloys and carbon steels. Acta Metall 7, 59-68.

Leblond, J.B. and Devaux, J., 1984. A new kinetic model for anisothermal metallurgical transformations in steels including the effect of austenite grain size. Acta Metall 32, 137-46.

van Es, S.H.J, Kolostein, M.H., Pijpers, R.J.M., Bijlaard, F.S.K., 2013, TIG-dressing of high strength steel butt welded connections – Part 1: weld toe geometry and local hardness. *Procedia Engineering* 66, 216 – 225.

van Es, S.H.J, Kolostein, M.H., Pijpers, R.J.M., Bijlaard, F.S.K., 2013, TIG-dressing of high strength steel butt welded connections – Part 2: physical modelling and testing. *Procedia Engineering* 66, 126 – 137.

Vemanaboina, H., Akella, S. and Buddu, R.K., 2014. Welding process simulation model for temperature and residual stress analysis. Procedia Materials Science 6, 1539 – 1546.

Williams, M.L., 1952. Stress singularities resulting from various boundary conditions in angular corners of plates in tension. *J Appl Mech* 19, 526–528.